IEEE Access
Multidisciplinary | Rapid Review | Open Access Journal

Received 4 July 2023, accepted 29 July 2023, date of publication 2 August 2023, date of current version 10 August 2023.

Digital Object Identifier 10.1109/ACCESS.2023.3301185

RESEARCH ARTICLE

High Isolated Four Element MIMO Antenna for ISM/LTE/5G (Sub-6GHz) Applications

SANTOSH KUMAR MAHTO[1], AJIT KUMAR SINGH[1], (Member, IEEE), RASHMI SINHA[2], (Member, IEEE), MOHAMMAD ALIBAKHSHIKENARI[3], (Member, IEEE), SALAHUDDIN KHAN[4], AND GIOVANNI PAU[5], (Member, IEEE)

[1]Indian Institute of Information Technology, Ranchi, Jharkhand 834010, India
[2]Department of ECE, National Institute of Technology, Jamshedpur, Jamshedpur, Jharkhand 831014, India
[3]Department of Signal Theory and Communications, Universidad Carlos III de Madrid, Leganés, 28911 Madrid, Spain
[4]College of Engineering, King Saud University, Riyadh 11421, Saudi Arabia
[5]Faculty of Engineering and Architecture, Kore University of Enna, 94100 Enna, Italy

Corresponding authors: Ajit Kumar Singh (ajitsingh31393@gmail.com), Mohammad Alibakhshikenari (mohammad.alibakhshikenari@uc3m.es), and Giovanni Pau (giovanni.pau@unikore.it)

Dr. Mohammad Alibakhshikenari acknowledges support from the CONEX-Plus programme funded by Universidad Carlos III de Madrid and the European Union's Horizon 2020 research and innovation programme under the Marie Sklodowska-Curie grant agreement No. 801538. The authors also sincerely appreciate funding from Researchers Supporting Project number (RSP2023R58), King Saud University, Riyadh, Saudi Arabia.

ABSTRACT A compact quad-port Multiple-Input-Multiple-Output (MIMO) antenna with an electrical dimension of $0.28\lambda_0 \times 0.28\lambda_0$ and impedance bandwidth of 5.03GHz (2.42-7.45GHz) is proposed. By combining a tapered feed line and stubs in the ground plane, which serve as open circuit stubs and whose dimensions are properly tuned to compensate for the antenna's input impedance, as the inductance and capacitance values are dependent on it, the bandwidth and isolation are improved. The MIMO antenna has a 15dB average isolation and a group delay $<$ 1nsec. In terms of the envelop correlation coefficient (ECC), diversity gain (DG), mean effective gain (MEG), and total active reflection coefficient (TARC), the proposed antenna's diversity performance characteristics are investigated, and the obtained values are 0.004, 9.99dB, $\pm$3dB, -10dB respectively. Further the channel capacity of the MIMO antenna is also calculated. The maximum channel capacity of the four elements is 21.34bits/sec./Hz. Equivalent circuit of the proposed MIMO is discussed in this article and S-parameter has been compared with simulated results and found good agreement between simulated and circuit results. A prototype was created to compare the calculated parameters with the measured ones to validate the suggested design. In addition, the scattering matrix, which includes the reflection coefficient (S11) and transmission coefficient (S21) between two elements, and other antenna parameters are all advantageous for applications in the Bluetooth (2.400-2.483GHz), ISM band (2.40-2.483GHz, 5.725-5.850GHz), WLAN/Wi-Fi, and 5G (sub-6GHz) bands.

INDEX TERMS MIMO antenna, 5G communication, channel capacity, isolation, mean effective gain (MEG), sub-6 GHz.

I. INTRODUCTION

It is critical in today's mobile communication environment to attain better data rates, capacity, and low latency. Fifth generation (5G) mobile communication has been implemented globally to attain the benefit [1], [2]. It has been demonstrated [3], [4], [5] that the MIMO antenna system should be used to boost information throughput for 5G operations. Because of the small size of the mobile terminal, achieving improved MIMO antenna system performance in terms of mutual coupling and ECC becomes a difficulty. The fundamental techniques for improving isolation and reducing interference in multi-antenna systems [6], [7], [8] typically include electromagnetic bandgap (EBG) architectures [9], [10], defected ground structure (DGS) [11], neutralization lines, engraved parasitic elements, metasurfaces

The associate editor coordinating the review of this manuscript and approving it for publication was Ali Karami Horestani.

(MTS) [12] and metamaterials (MTM) [13]. Mutual coupling can be manipulated using these ways by weakening, resisting, or lowering the surface current flow [14].

In the literature, several MIMO antennas [15], [16], [17], [18], [19], [20], [21], [22], [23], [24], [25] have been designed for multiple wireless applications. Small size broadband circularly polarized (CP) two-element MIMO slot antenna was proposed in [15]. The antenna obtained a bandwidth of 3.17-17.39GHz with an electrical dimension of $0.42\lambda_0 \times 0.22\ \lambda_0 mm^2$. Four element MIMO antenna with a bandwidth of 1.66-2.17GHz was proposed for LTE application [16]. The dimension of the antenna was $0.38\lambda_0 \times 0.54\ \lambda_0 mm^2$with isolation $>$ 12dB at a lower frequency of 1.66GHz. In [17], a four-port rectangular radiator was proposed for 5.7GHz wireless applications. Isolation of more than 13dB was achieved without using a decoupling structure. A four-port MIMO antenna for 2.4GHz Wi-Fi applications was discussed in [18]. A decoupling structure was used to improve mutual coupling. The electrical dimension of proposed structure was $0.56\lambda_0 \times 0.56\ \lambda_0 mm^2$and isolation $>$ 13dB. In [19], a wide-band MIMO antenna was proposed for Wi-Fi-LTE, wireless access point (WAP) application with an impedance bandwidth of 0.6GHz. The proposed antenna had two common elements with an L-corner ground plane. In [20], a compact WLAN band rejection MIMO antenna was proposed with four ports and a common ground plane and has an electrical dimension of $0.45\lambda_0 \times 0.36\ \lambda_0 mm^2$with ECC of 0.002. A four-port MIMO antenna system with a frequency range of 3.2–5.75 GHz has been proposed for use in 5G new radio (NR) sub-6 GHz WLAN applications [21]. The antenna elements are orthogonally oriented to each other with spacing of $0.3\lambda_0$ between elements. Ultra-wideband MIMO antenna based on the compact coplanar waveguide (CPW) method was presented in [22]. The suggested MIMO antenna design has four jug-shaped radiating elements to make it ultra-wideband. Four orthogonally positioned antenna elements were used to realise the polarisation diversity phenomena. [23] introduced a miniature circularly polarised MIMO antenna for wearable biotelemetric systems. Four elements make up the proposed MIMO antenna, which are arranged orthogonally to one another. A two-element slotted octagon-shaped antenna for 5G applications that operates in the sub-6 GHz spectrum (3.1-4.5 GHz) was discussed in [24]. To reduce mutual coupling between MIMO antennas, a T-formed isolation structure is positioned at a ground plane. A small, three Sub-6 GHz 5G band, four element MIMO antenna has been proposed in [25]. With the coupled ground at the back, the four element MIMO antenna obtains a symmetric structure on top. The suggested FR-4-based device operates in the frequency bands of 3.72–6.46 GHz with a tiny size of $0.39\lambda_0^2$(f_0 = 3.72 GHz) and requires no additional isolation element.

Contributions- The main contributions of this work are summarized as follows-

- A miniaturized MIMO antenna is proposed for Bluetooth, ISM, and 5G (sub-6GHz) applications as shown in Table 1.
- We have drawn the equivalent circuit diagram of the proposed antenna and verified the S11 with the antenna results.
- In this article, we have also calculated the channel capacity, which is an important parameter for the MIMO antenna.
- In this proposed article, by adding a stub in the ground plane, isolation has been improved up to 40dB.

A compact 2 × 2 MIMO antenna with an electrical dimension $0.28\lambda_0 \times 0.28\lambda_0 mm^2$ is proposed in this article. The 5.03GHz bandwidth and isolation are achieved with a tapered feed and a portion of the ground plane connected by stubs. The suggested antenna has a 15dB average isolation over the operating band with ECC $<$ 0.004, a peak gain of 4.2dBi, and an average overall efficiency of 90%. The proposed antenna focuses on multiple wireless applications such as Bluetooth (2.400-2.483GHz), ISM band (2.40-2.483GHz, 5.725-5.850GHz) WLAN/Wi-Fi, and 5G (sub-6GHz) range. For bluetooth and ISM band applications, the proposed antenna offers wide impedance bandwidth with good return loss, radiation properties and group delay $<$ 1nsec. The measurement results show that the antenna might be simply integrated with the bluetooth and ISM band applications existing circuit.

II. DESIGN

The proposed compact MIMO antenna is comprised of four-square radiators and a partial ground plane with rectangular stubs, as shown in Fig. 1. Its overall dimensions are $35 \times 35 \times 1.6\ mm^3$ and it is constructed on a low cost FR4 substrate with a ε_r of 4.4 and a loss tangent of 0.02. Tapered microstrip feed lines and rectangular stubs in the ground plane, which serve as open circuit stubs and whose dimensions are properly tuned to compensate for the antenna's input impedance, as the inductance and capacitance values are dependent on it, can be used to improve matching and isolation. By changing the dimensions (a & b) of the stub, the desired bandwidth of the suggested MIMO antenna can be attained. center-to-center (CTC) spacing in a MIMO system is 22 mm (0.18 λ_0), (where $\lambda_0$determined at the lower cut off frequency of 2.42GHz. To reduce the coupling between elements, the MIMO model uses a multiple ground plane. As the MIMO antenna does not have a shared ground plane, the antenna's reliability is lowered because its behaviour can differ between devices. To address it, multiple ground planes of MIMO antenna components are associated unitedly with $0.5 \times 1mm^2$ of connecting strips to form a shared ground as portrayed in Fig. 1 [26].

The optimized parameters of the proposed antenna are:

L_S =W_S =W_g =35mm, L_g =5, W_P =L_P =6mm, W_f =1.6mm, L_f =9mm, s=0.7mm, a=12mm, b=7mm, c=0.5mm, d=1mm.

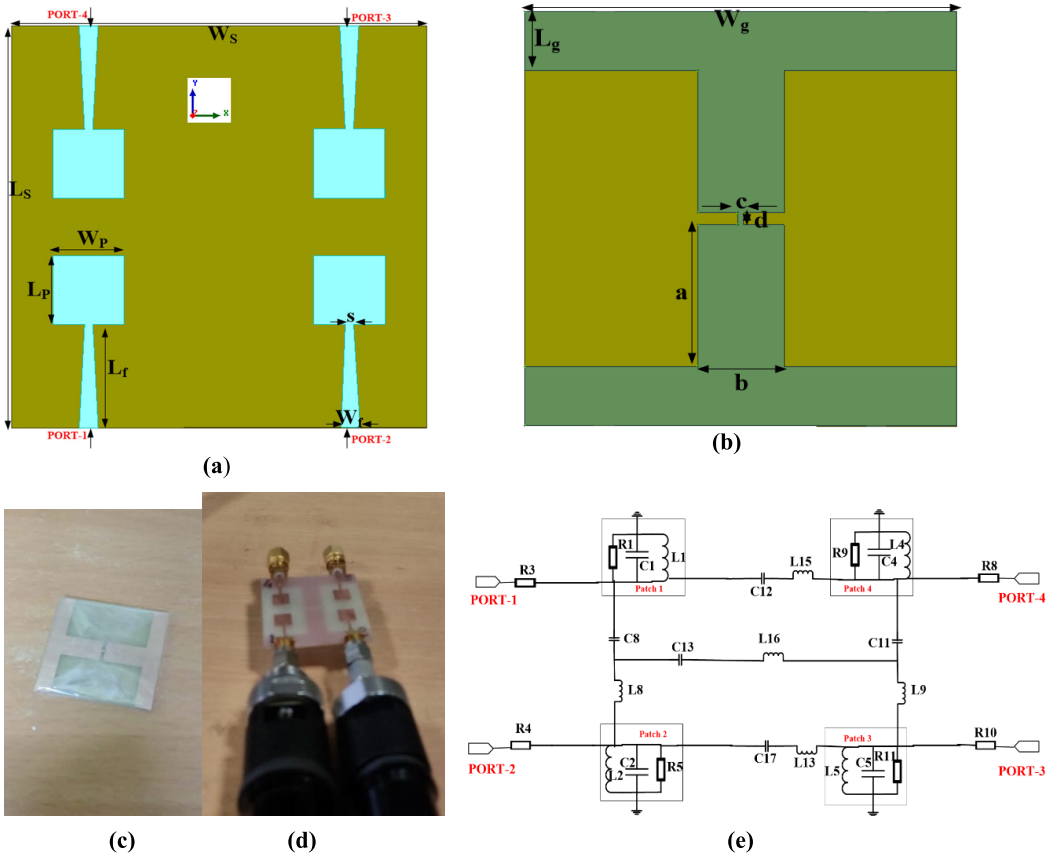

FIGURE 1. Proposed MIMO antenna (a) Front view (b) Back view, (c) Fabricated (Back View) (d) Measurement setup of MIMO Antenna (e) Equivalent circuit diagram.

Initially, a rectangular fed single square patch of dimension 6mm×6mm with a fully ground plane is considered as shown in Fig. 2(a) and corresponding S11 is shown in Fig. 2(g). [27]. When considering rectangular and tapered feed with full ground plane, as illustrated in Figs. 2(a)-(b), the impedance matching is not adequate. In addition, Fig. 2(c) displays the tapered fed with partial ground plane. Impedance, group delay and reflection coefficient plot of tapering fed with partial ground of single element are shown in Figs. 2(h), 2(i), and 2(g) respectively. The graph makes clear that the impedance is nearly 50Ω (4.12-4.55GHz) with a partial ground plane. Group delay performs well in the designated band as well. Further two elements with stub and without MIMO antenna are designed as shown in Figs. 2(d)- (e) and finally quad element MIMO antenna is shown in Fig. 2(f). From Fig. 2(g), it is visible that proposed frequency range is achieved with dual and quad element MIMO antenna.

Instead of using a fully-ground plane, a partial ground plane is used, and 1 × 2 and 2 × 2 MIMO antenna are designed. The reflection and transmission coefficient of a two-element MIMO antenna are shown in Fig. 3. Matching is accomplished at some frequency ranges (3.2-4.6GHz) when the rectangular fed without stub is considered, while isolation is not satisfactorily accomplished because in operating frequency range mutual coupling is less than 10dB as shown in Fig. 3(b). Further rectangular fed with stub, matching achieved from 4.3-5.1GHz as shown in Fig. 3(a) along with average isolation 22dB as shown in Fig. 3(b), but lower frequency range could not be achieved. Tapered fed without stub matching did not fetch in the operating frequency range. In the last tapered fed with stub matching is achieved from 4.1-6.9GHz and isolation are also good in the operating frequency range as shown in Fig. 3(b). Therefore, it concludes that isolation is improved by adding a stub in the ground plane either by rectangular fed or tapered fed. Further to achieve the lower frequency range, a 2 × 2 MIMO antenna is proposed. Utilizing a tapered microstrip feed line increases the operation bandwidth of 5.03GHz (2.42-7.45GHz). A tapered connection between the feed line and the main patch is applied to smooth the current's path, thus providing wider impedance bandwidth. A tapered feed region is optimised such that 50Ω impedance matching is done properly to reduce the reflection of the incident waves. The tapered feed line along with the printed travelling wave antennas exhibits wideband characteristics and is capable of transmitting UWB pulses with low distortions. By utilising a rectangular stub in the partial ground plane, isolation is increased up to 40dB over the operational band (2.42-7.45GHz). Additionally, this stub offers a decoupling path, which limits the amount of current that couples to the neighbouring element due to surface waves, keeping it below -10 dB over the whole target frequency range.

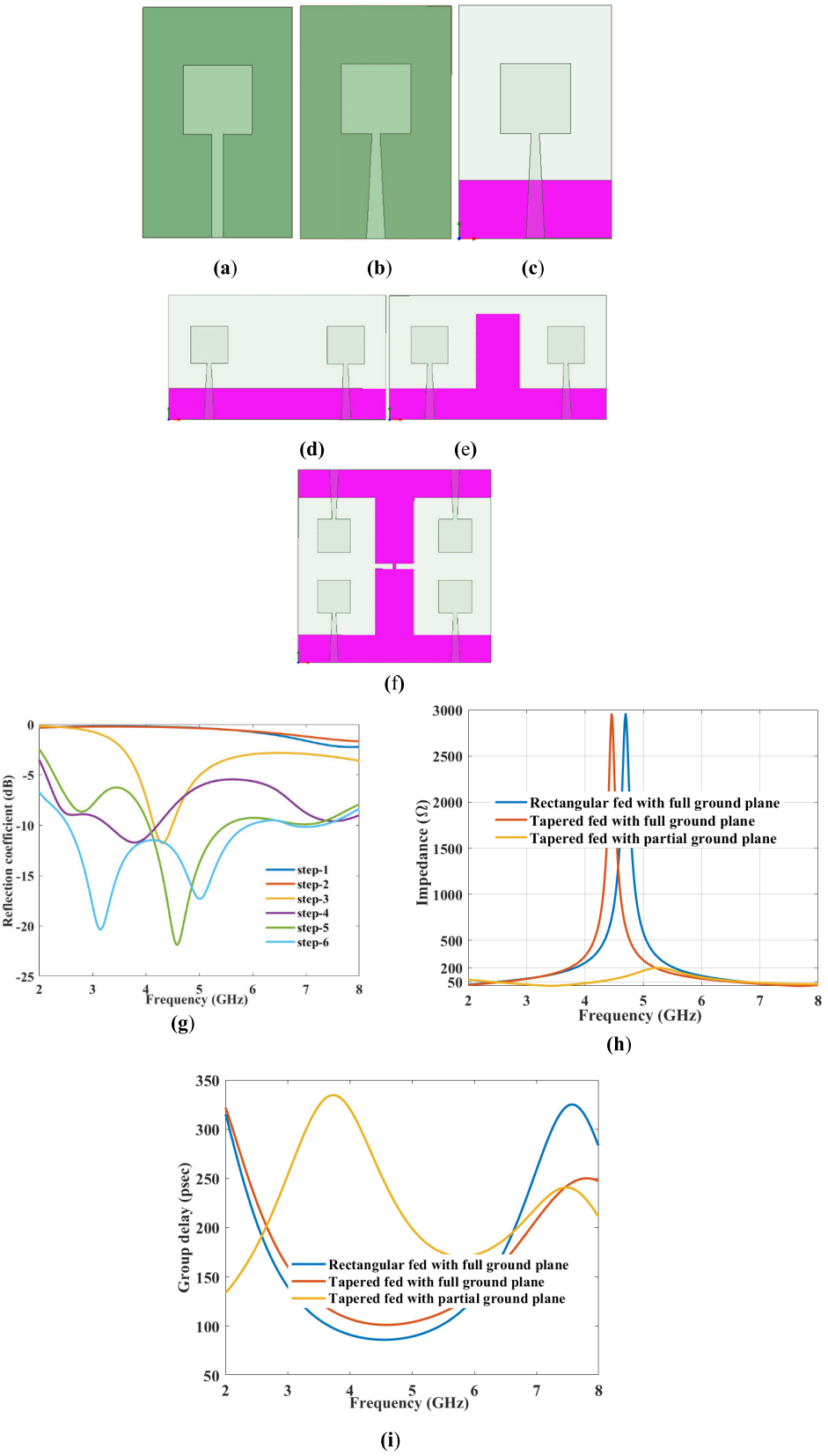

FIGURE 2. Antenna evolution (a) step-1 (rectangular fed with full ground plane), (b) step-2 (tapered fed with full ground plane) (c) step-3 (tapered fed with partial ground plane) (d) step-4 (dual element without stub) (e) step-5 (dual element with stub (f) step-6 (proposed antenna) (g) Reflection coefficient (h) Impedance plot (i) Group delay.

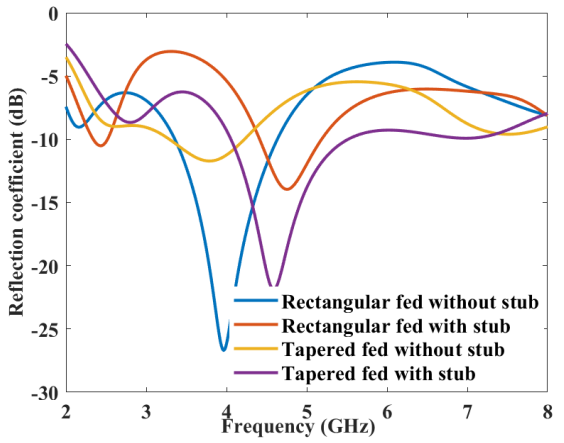

(a)

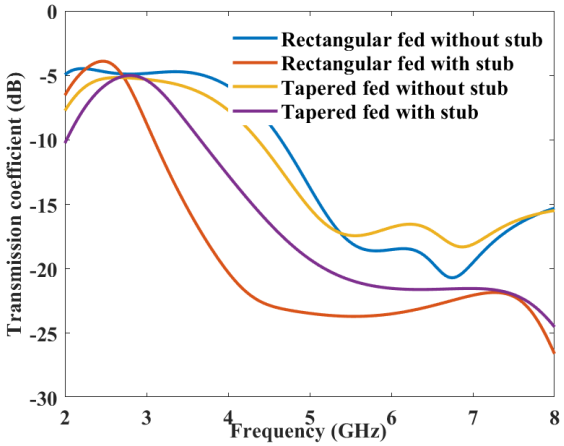

(b)

FIGURE 3. Dual element antenna (a) Reflection coefficient (b) Transmission coefficient.

Equivalent circuits are used to evaluate its electrical behaviour in response to an input RF signal. Fig. 1(e) addresses the equivalent circuit model of quad element MIMO antenna, where four patches are shown with circuit resistances (R_1, R_5, R_9, and R_{11}), capacitances (C_1, C_2, C_4, and C_5), and inductances (L_1, L_2, L_4, and L_5). Coupling between the elements is due to inductance and capacitance that depends on it. The strip between two stubs is represented by L_{16} & C_{13} and between adjacent elements coupling represented by $L_8, C_8, L_9, C_{11}, L_{13}, C_{17}$, and L_{15}, C_{12} respectively.

III. PARAMETRIC ANALYSIS

By varying ground length and width, feed length and width, spacing (s), stub length (a) and width (b), and patch dimensions, the parametric study of reflection coefficient (S11) and group delay has been performed.

Group delay- It refers to phase distortion between transmitted and received signals.

$$\tau_g(\omega) = -\frac{d\varphi(\omega)}{d\omega} = -\frac{d\varphi(f)}{2\pi df} \quad (1)$$

in which Ø(f), Ø is the frequency-dependent phase of the radiated signal. The group delay fluctuations caused by the antenna's radiation pattern will have an impact on the overall receiver system performance since they can cause severe timing errors.

S11, S12 and group delay are investigated by adjusting L_g from 4mm to 6mm as shown in Fig. 4(a), Fig. 4(b) and Fig. 4(g) respectively, and the optimum length is achieved at 5mm. At L_g =4mm, S11 is not good, and group delay exceeds 1nsec, however for L_g =6mm, group delay and isolation are good while S11 is above 10dB from 5.8-6.2GHz frequency range.

S11, isolation and group delay are presented in Fig. 4(c), Fig. 4(d), and Fig. 4(h) respectively, as a function of stub dimensions. The optimum bandwidth, isolation and group delay are attained at a=12mm and b=7mm, as can be observed. Now, by varying W_f from 1.5mm-1.7mm and spacing (s) from 0.6mm-0.8mm as shown in Figs. 4(e) and 4(f) and 4(i) respectively. The optimum results are obtained at W_f =1.5mm and s=0.8mm & W_f =1.6mm, and s=0.7mm. However, the ECC is less in the case of W_f =1.6mm, and s=0.7mm.

The group delay is shown in Figs. 4(g)-(i). From the graph, a steady group delay < 1ns is acquired over the entire frequency range (2.42–7.45 GHz). If the group delay variation exceeds 1 ns, a pulse distortion is caused because phases are non-linear in the far-field region [28].

The parametric analysis of ground plane width (W_g) is depicted in Fig. 4(j). At W_g =33mm, S11 is exceeding -10dB, although it is close to -10dB at W_g =34mm. The optimum bandwidth is acquired at W_g =35mm. Further, by varying the patch dimensions as shown in Figs. 4(k) and 4(l), the optimum matching is obtained at L_P =W_P =6mm. Now, by adjusting the length of the feed line (L_f) from 7mm-9mm, the optimum result is obtained at L_f =9mm. As L_f increases, resonance frequency-shifted towards lower frequency [29] as shown in Fig. 4(m).

IV. RESULTS AND DISCUSSION

The proposed antenna's simulated and experimental S-parameter characteristics, shown in Figs. 5(a) – (b) are < -10dB and -10dB, respectively, over the entire frequency range. The maximum measured return loss is obtained at -21dB at 2.9GHz, whereas minimum isolation -10dB at 2.74GHz frequency. At some frequency there are discrepency in simulated and experimental results due to human errors and fabrication tolerances. Fig.5(c) represents the measured and simulated group delay, and from figure it is visible that group delay is < 1nsec. The simulated S-parameters and circuit analysis are shown in Figs. 5(d) – (e). Using circuit analysis, at some frequency S11 is exceeding -10dB, due to improper matching at frequency band.

The peak gain of the MIMO at all ports is shown in Fig. 6(a). The antennas average peak gain is 2.72dBi. The total efficiency of the antenna is displayed in Fig. 6(b). Throughout the entire bandwidth, the average total efficiency

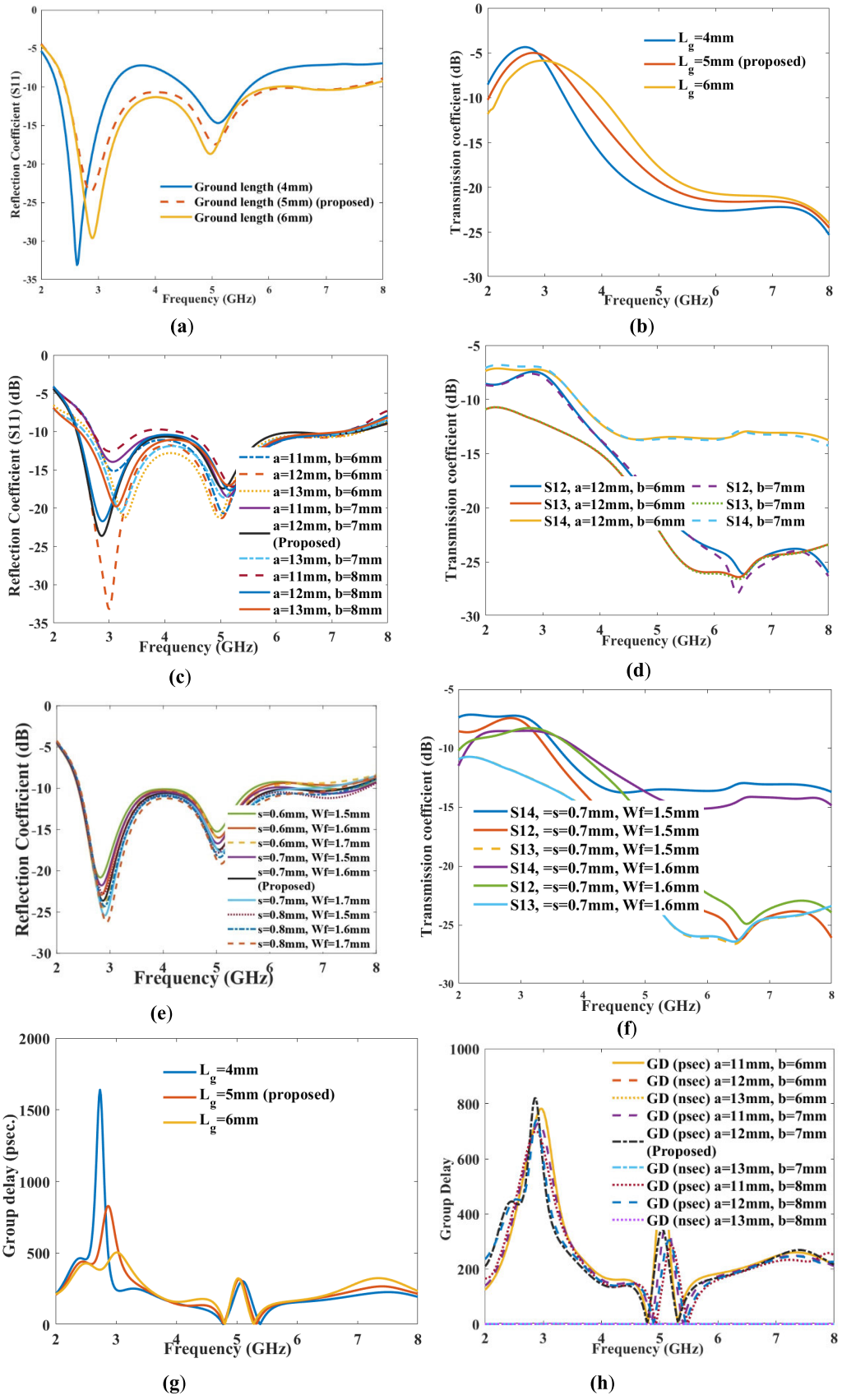

FIGURE 4. Parametric analysis of proposed antenna.

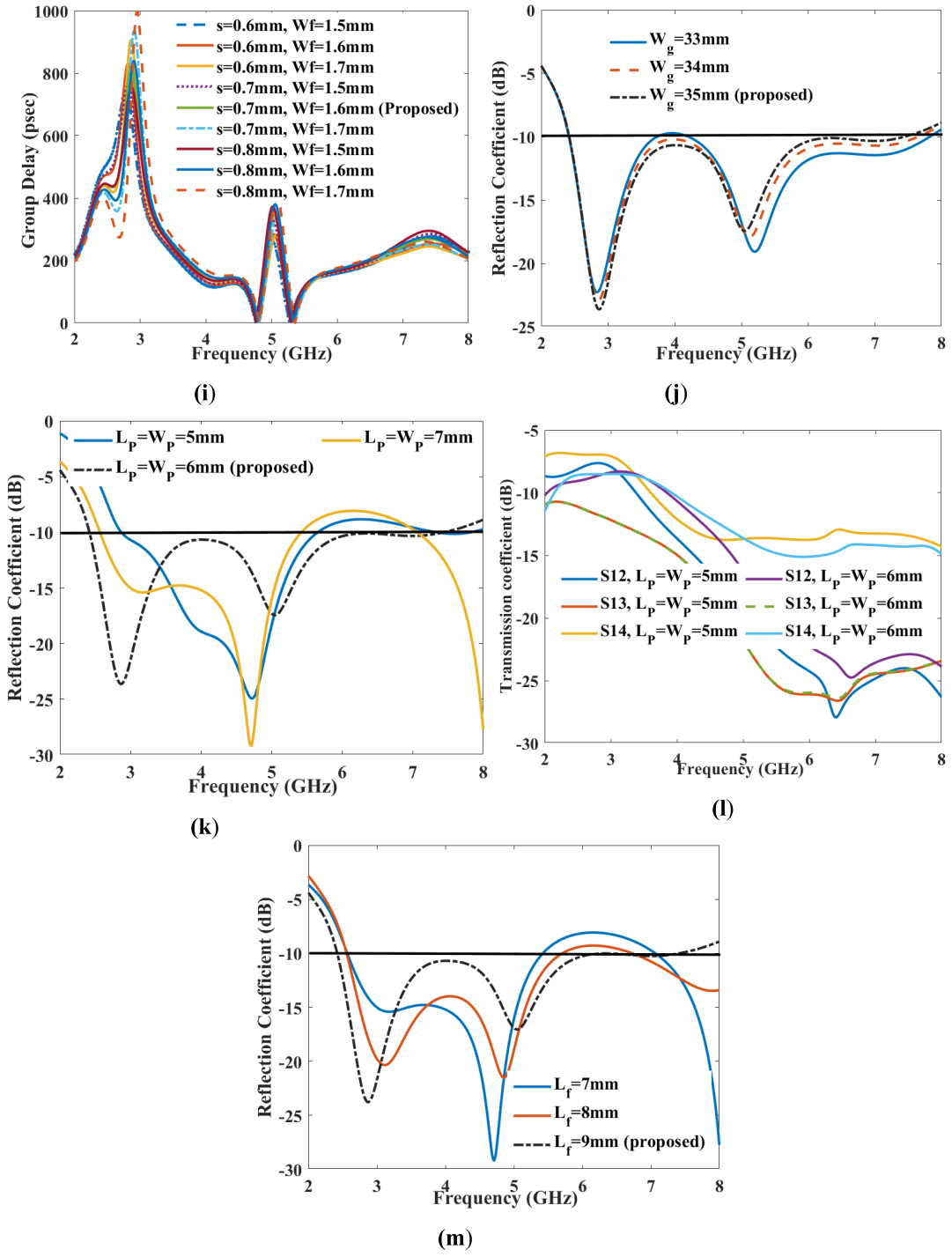

FIGURE 4. *(Continued.)* **Parametric analysis of proposed antenna.**

is 90% (-0.90dB). It may be deduced from the figure that the suggested antenna performs well across the whole range. Measurement of total efficiency is done by the following equation [30]-

$$\eta_{\text{total}}\,(\text{port}-1)=\eta(1-|S_{11}|^2-|S_{21}|^2) \tag{2}$$

where the radiation efficiency is denoted by η. The ratio of the total power radiated (P_r) to the total power accepted at its input terminal (P_a) is known as the antenna's radiation efficiency.

$$\eta=\frac{P_r}{P_a} \tag{3}$$

where-

$$P_a=(1-|\Gamma|^2)P_S \tag{4}$$

A power metre (or a receiver) can be used to measure the power delivered to the antenna (P_s), and a vector network analyzer can be used to measure the reflection coefficient (Γ).

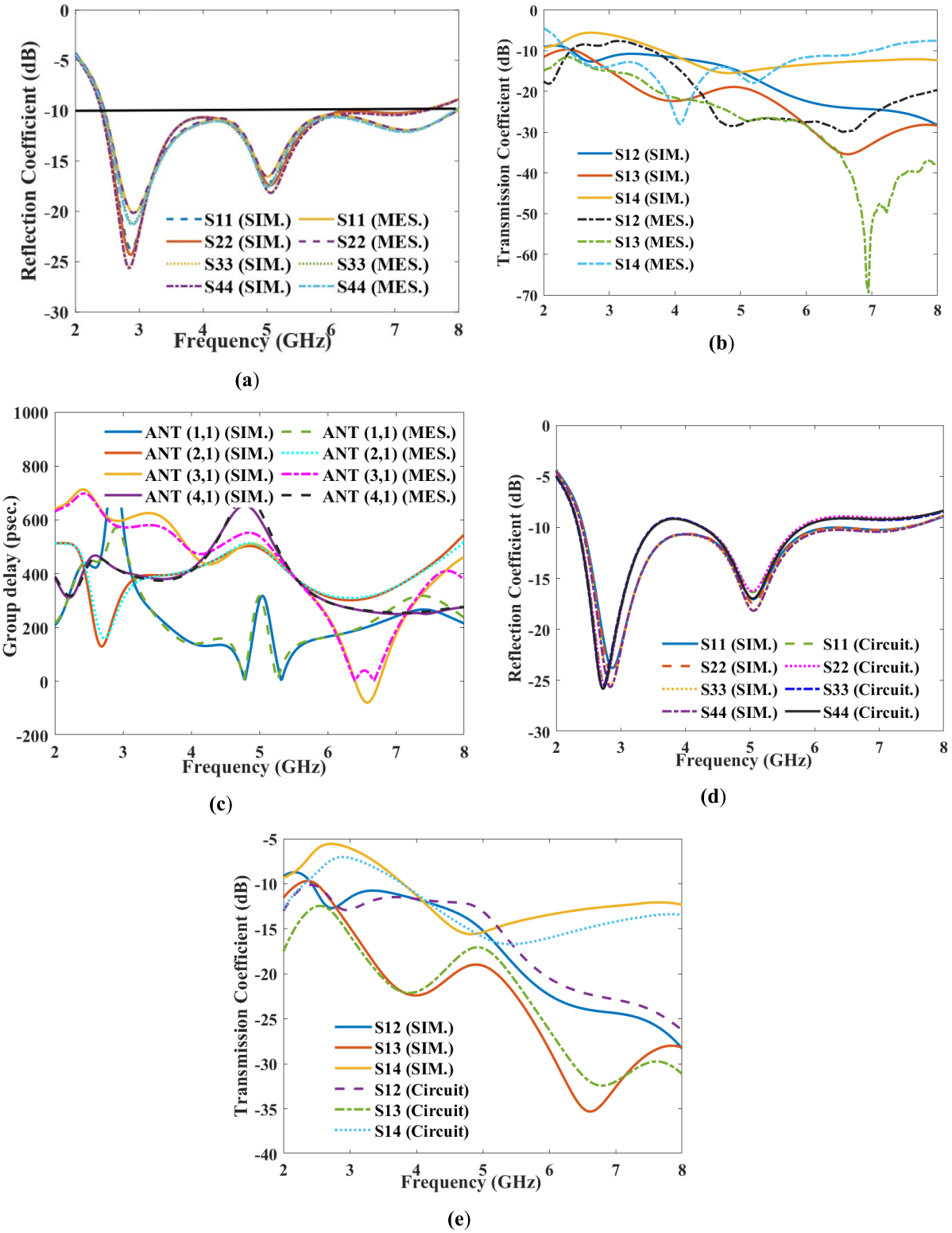

FIGURE 5. S-parameter characteristics (a) Reflection coefficient (b) Transmission coefficient (c) Group delay (d) Reflection coefficient with circuit (e) Transmission coefficient with circuit.

At 2.48GHz and 3.5GHz frequencies, respectively, 2D radiation patterns are shown in Figs. 6(c) & (d), and it is noted that designs are practically omnidirectional at Ø= 90^0 and resemble dipoles at Ø = 0^0.

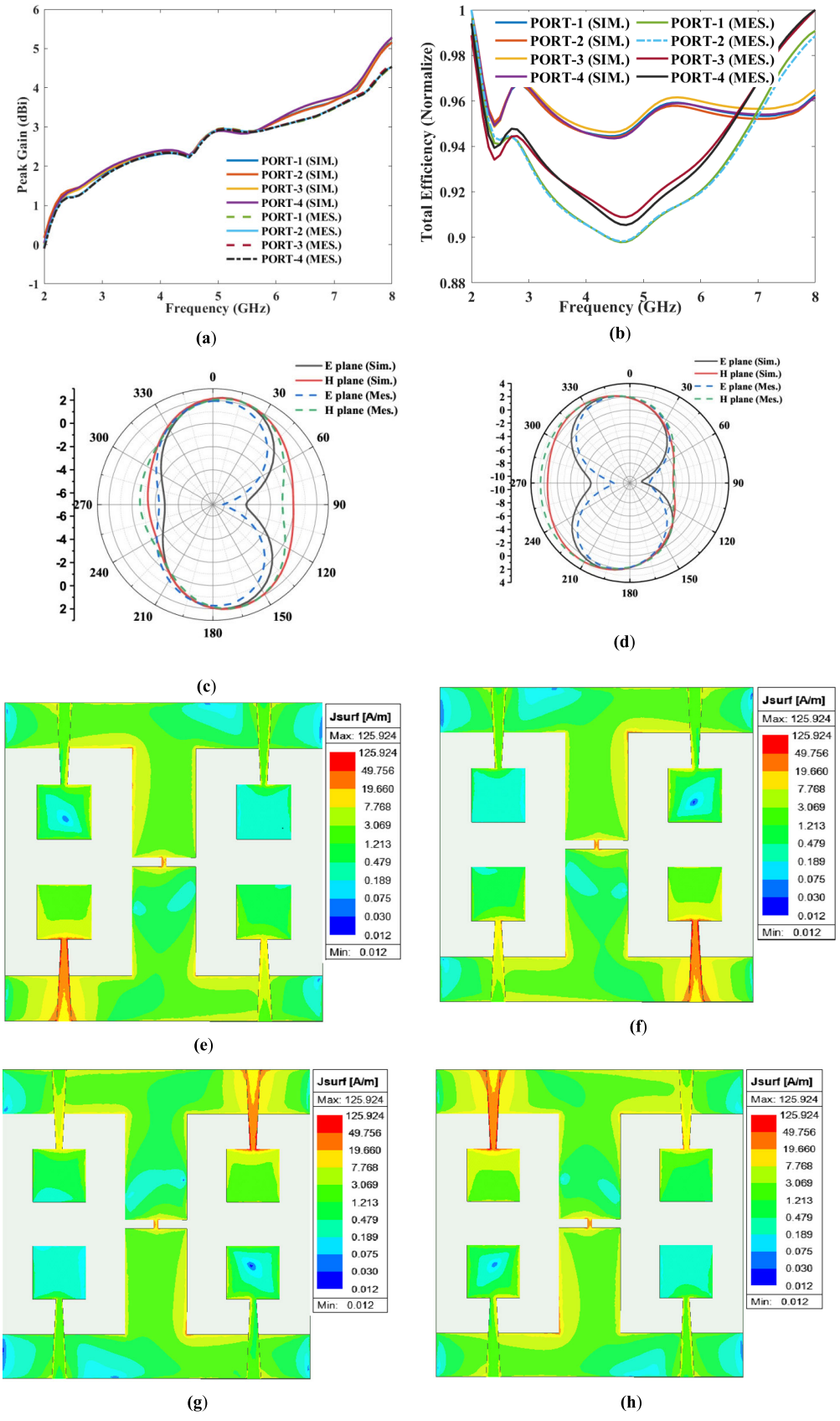

FIGURE 6. (a) Peak Gain (b) Total Efficiency (c) E & H plane at (c) 2.48GHz (d) 3.5GHz (e) Surface current at 3.5GHz (e) PORT-1 (f) PORT-2 (g) PORT-3 (h) PORT-4.

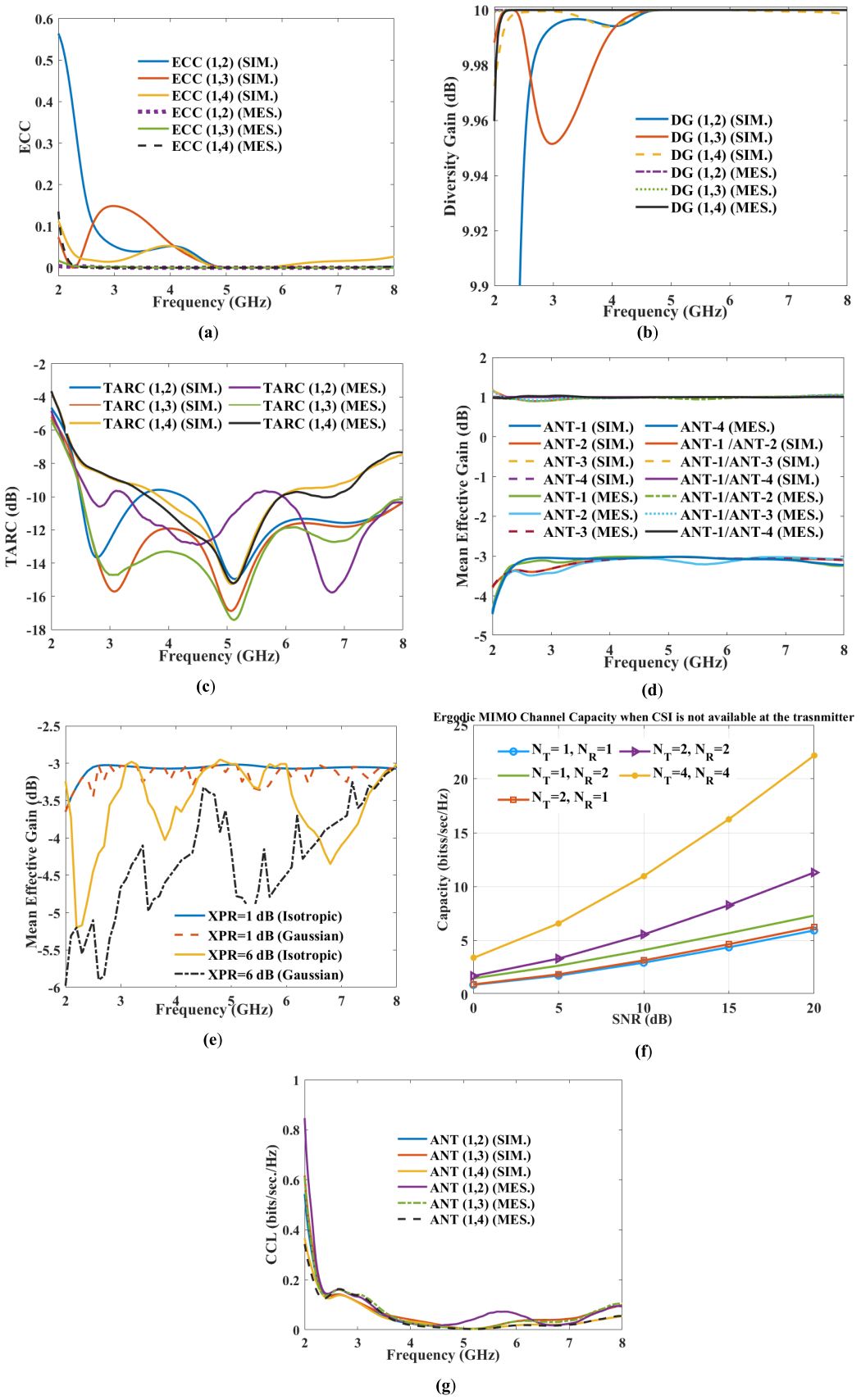

FIGURE 7. (a) ECC (b) DG (c) TARC (d) MEG (e) MEG vs frequency in different medium (f) Ergodic capacity (g) CCL.

TABLE 1. Comparative chart with other mimo antenna.

Ref.	Electrical Size(mm^2)	No. of radiation elements	Frequency range (GHz)	Isolation (dB)	ECC	Decoupling principle	Design complexity
15	$0.42\lambda_0\times0.22\lambda_0$	2	3.17-17.39	>16	0.005	Metal strip slot	Complex
16	$0.38\lambda_0\times0.54\lambda_0$	4	1.66-2.17	>12	0.23	No decoupling technique	Simple
17	$1.1\lambda_0\times1.1\lambda_0$	4	4.4-6.4	>13	0.04	Orthogonal arrangement of ports	Complex
18	$0.56\lambda_0\times0.56\lambda_0$	4	2.34-2.56	10-14	0.01	Diagonal parasitic element	Complex
19	$0.8\lambda_0\times0.96\lambda_0$	2	2.3-2.9	>15	0.15	Parasitic element	Complex
20	$0.45\lambda_0\times0.36\lambda_0$	4	2.7-5.1,5.9-12	>17	0.002	Orthogonal arrangement	Complex
21	$0.50\lambda_0\times0.50\lambda_0$	4	3.2-5.75	>15	0.002	Orthogonal arrangement	Complex
22	$0.60\lambda_0\times0.60\lambda_0$	4	3-11	>16	0.02	Orthogonal arrangement	Complex
23	$0.67\lambda_0\times0.67\lambda_0$	2	1.8-3.1	>16	0.2	G-shaped ground plane on each element	Complex
24	$0.57\lambda_0\times0.4\lambda_0$	2	3.1-4.5	>15	0.004	T-shaped structure in the ground plane	simple
25	$0.39\lambda_0\times0.39\lambda_0$	4	3.72-6.46	>15	0.1	No decoupling technique	Complex
[P]	**$0.28\lambda_0\times0.28\lambda_0$**	**4**	**2.42-7.45**	**>12**	**0.004**	**Using stub**	**Simple**

The surface current analysis of a MIMO antenna at 3.5GHz frequency is displayed in Fig. 6(e). The main reason for mutual coupling between close antenna elements is the transfer of surface currents from the stimulated port-1 to port-4, as shown in Fig. 6(e). The stimulation of one port and the termination of another port with matched load causes a low surface current in other ports. The maximum surface current is concentrated on the feed line. Fraction of currents is also

visible to other ports as well because of the partial ground plane, which can be neglected. A very less current on other ports shows that the proposed decoupling technique is suitable for the proposed MIMO antenna.

V. MIMO DIVERSITY PERFORMANCE

The diversity features are utilised to test the effectiveness and capability of the MIMO antenna.

The ECC which considers radiation pattern, polarization, and relative phase of the fields can be calculated using (5) [31]

$$|\rho_e(i,j,N)| = \frac{\sum_{n=1}^{N} S_{i,n}^{*} S_{n,j}}{\prod_{k(=i,j)} [\sum_{n=1}^{N} S_{i,n}^{*} S_{n,k}]} \tag{5}$$

Here, consider the values of i, j, N = 1 to 4 (for four elements).

DG is calculated as follows:

$$DG = 10\sqrt{1 - ECC^2} \tag{6}$$

The ideal value of DG is 10dB.

As shown in Figs. 7(a) and (b), the computed ECC and DG are < 0.004 and 9.99dB, respectively, indicating good diversity performance.

TARC is a significant metric in quad-port antennas since it shows the relationship between radiated and received power. The TARC may be determined using (7) [32],

$$TARC = \frac{\sqrt{(S_{11} + S_{12})^2 + (S_{21} + S_{22})^2}}{\sqrt{4}} \tag{7}$$

TARC $<$ 0dB for MIMO antenna in ideal condition. As displayed in Fig. 7(c), the TARC measured value is <-15dB.

MEG is a metric for calculating the median power from the event power [33]. For two elements, MEG is calculated by (8) and (9) and displayed in Fig. 7(d).

$$MEG_i = 0.5\left[1 - \sum_{j=1}^{N} |S_{ij}|^2\right] < -3dB \tag{8}$$

$$MEG_j = 0.5\left[1 - \sum_{i=1}^{N} |S_{ij}|^2\right] < -3dB \tag{9}$$

$$|MEG_i - MEG_j| < 3dB \tag{10}$$

$$\left|\frac{MEG_i}{MEG_j}\right| = \pm 3dB \tag{11}$$

As shown in Fig. 7(e) [33], mean effective gain is calculated using far field in both outdoor and indoor medium.

$$MEG_i = \oint [\frac{XPR \times G_{\theta i}(\Omega) + G_{\emptyset i}(\Omega) \times P_{\emptyset}(\Omega)}{1 + XPR}] d\Omega \tag{12}$$

In which XPR represents the cross-polarization ratio. The power density functions of the incident wave is $P_{\Phi}(\Omega)$ and $G_{\theta i}(\Omega)$, $G_{\Phi i}(\Omega)$ are the power gain, Ω represent the beam area. The value of i is 1 to 4 for four elements.

The performance of the MIMO system is determined using channel capacity which is proportional to bandwidth and signal to noise ratio (SNR). Equal power is given to the transmitting antenna element. The Ergodic MIMO channel capacity for four element antenna is calculated by using (13) [34] and shown in Fig. 7(f),

$$C_{2\times 2MIMO(Max.)} = n(b[log_2[\det([I] + \frac{SNR}{n}[H]\left[H^*\right])]] \tag{13}$$

where [H], [H*] signify identity matrix, n is the number of antenna elements. Here we have considered that transmitter has no channel state information (CSI) and equal power has given to all antenna elements.

The channel capacity loss (CCL) for a two-element MIMO antenna is determined using equation (14) [35], as illustrated in Fig. 7(g).

$$CCL = -\log_2 det[\beta^R] \tag{14}$$

where, $[\beta^R] = \begin{bmatrix} \beta_{ii} & \beta_{ij} \\ \beta_{ji} & \beta_{jj} \end{bmatrix}$

$$\beta_{ii} = 1 - (\sum_{j=1}^{N} |S_{ij}|^2) \tag{15}$$

$$\beta_{ij} = -\left(S_{ii}^{*} S_{ij} + S_{ji}^{*} S_{ij}\right) \tag{16}$$

The comparative study of the MIMO antenna is shown in Table 1. The antenna has a size of $0.28\lambda_0 \times 0.28\lambda_0$, which is more compact than other antenna dimensions. As indicated in Table 1, the measured value of ECC is 0.004, except [20], [21]. The isolation of the MIMO antenna is 15dB, which is better than [16], [17], and [18], however, less than [15], [20], [21], [22], and [23]. The antenna's overall average efficiency is a respectable 90%. Therefore, it can be said that the suggested antenna has the necessary properties to be used for LTE/5G bands.

VI. CONCLUSION

A compact MIMO antenna for Bluetooth/ISM/LTE/5G bands is designed, fabricated, and measured. The simulated results have close agreement with the fabricated MIMO antenna. S-parameters far filed radiation characteristics, and diversity performance of the MIMO antenna are analyzed and discussed in this article. Therefore, it is suggested as a suitable aspirant for Bluetooth (2.400-2.483GHz), ISM band (2.40-2.483GHz, 5.725-5.850GHz), WLAN/Wi-Fi, and 5G (sub-6GHz) applications. Further applications of MIMO array can be used in mobile radio telephones such as 3GPP and 3GPP2, HSPA+LTE, and sensing problems. It can also be used in non-wireless communications systems like home networking standard ITU-T G.9963.

ACKNOWLEDGMENT

Dr. Mohammad Alibakhshikenari acknowledges support from the CONEX-Plus programme funded by Universidad Carlos III de Madrid and the European Union's Horizon 2020 research and innovation programme under the Marie Sklodowska-Curie grant agreement No. 801538. The authors also sincerely appreciate funding from Researchers Supporting Project number (RSP2023R58), King Saud University, Riyadh, Saudi Arabia.

REFERENCES

[1] M. Agiwal, A. Roy, and N. Saxena, "Next generation 5G wireless networks: A comprehensive survey," *IEEE Commun. Surveys Tuts.*, vol. 18, no. 3, pp. 1617–1655, 3rd Quart., 2016.

[2] M. J. Marcus, "5G and 'IMT for 2020 and beyond' [spectrum policy and regulatory issues]," *IEEE Wireless Commun.*, vol. 22, no. 4, pp. 2–3, Aug. 2015.

[3] M. N. Hasan, S. Bashir, and S. Chu, "Dual band omnidirectional millimeter wave antenna for 5G communications," *J. Electromagn. Waves Appl.*, vol. 33, no. 12, pp. 1581–1590, Aug. 2019.

[4] D. Singh, A. A. Khan, S. A. Naqvi, M. S. Khan, A.-D. Capobianco, S. Boscolo, M. Midrio, and R. M. Shubair, "Inverted-c ground MIMO antenna for compact UWB applications," *J. Electromagn. Waves Appl.*, vol. 35, no. 15, pp. 2078–2091, Oct. 2021.

[5] Y.-L. Ban, C. Li, C.-Y.-D. Sim, G. Wu, and K.-L. Wong, "4G/5G multiple antennas for future multi-mode smartphone applications," *IEEE Access*, vol. 4, pp. 2981–2988, 2016.

[6] M. Li, Y. Zhang, D. Wu, K. L. Yeung, L. Jiang, and R. Murch, "Decoupling and matching network for dual-band MIMO antennas," *IEEE Trans. Antennas Propag.*, vol. 70, no. 3, pp. 1764–1775, Mar. 2022.

[7] M. Li, L. Jiang, and K. L. Yeung, "A novel wideband decoupling network for two antennas based on the Wilkinson power divider," *IEEE Trans. Antennas Propag.*, vol. 68, no. 7, pp. 5082–5094, Jul. 2020.

[8] M. Alibakhshikenari, F. Babaeian, B. S. Virdee, S. Aïssa, L. Azpilicueta, C. H. See, A. A. Althuwayb, I. Huynen, R. A. Abd-Alhameed, and F. Falcone, "A comprehensive survey on 'various decoupling mechanisms with focus on metamaterial and metasurface principles applicable to SAR and MIMO antenna systems,'" *IEEE Access*, vol. 8, pp. 192965–193004, 2020.

[9] M. Alibakhshikenari, B. Virdee, P. Shukla, C. See, R. Abd-Alhameed, M. Khalily, F. Falcone, and E. Limiti, "Antenna mutual coupling suppression over wideband using embedded periphery slot for antenna arrays," *Electronics*, vol. 7, no. 9, p. 198, Sep. 2018.

[10] M. Alibakhshikenari, M. Khalily, B. S. Virdee, C. H. See, R. A. Abd-Alhameed, and E. Limiti, "Mutual coupling suppression between two closely placed microstrip patches using EM-bandgap metamaterial fractal loading," *IEEE Access*, vol. 7, pp. 23606–23614, 2019.

[11] C.-Y. Chiu, C.-H. Cheng, R. D. Murch, and C. R. Rowell, "Reduction of mutual coupling between closely-packed antenna elements," *IEEE Trans. Antennas Propag.*, vol. 55, no. 6, pp. 1732–1738, Jun. 2007.

[12] M. Alibakhshikenari, C. H. See, B. Virdee, and R. A. Abd-Alhameed, "Meta-surface wall suppression of mutual coupling between microstrip patch antenna arrays for THz-band applications," Tech. Rep., 2018.

[13] M. Alibakhshikenari, B. S. Virdee, C. H. See, R. A. Abd-Alhameed, F. Falcone, and E. Limiti, "Surface wave reduction in antenna arrays using metasurface inclusion for MIMO and SAR systems," *Radio Sci.*, vol. 54, no. 11, pp. 1067–1075, Nov. 2019.

[14] M. Li, J. M. Yasir, K. L. Yeung, and L. Jiang, "A novel dual-band decoupling technique," *IEEE Trans. Antennas Propag.*, vol. 68, no. 10, pp. 6923–6934, Oct. 2020.

[15] M. M. Sharma and R. P. Yadav, "Broadband circularly polarized compact MIMO slot antenna based on strip and stubs for UWB applications," *Electromagnetics*, vol. 41, no. 3, pp. 185–195, Apr. 2021.

[16] L. Malviya, R. K. Panigrahi, and M. V. Kartikeyan, "Four element planar MIMO antenna design for long-term evolution operation," *IETE J. Res.*, vol. 64, no. 3, pp. 367–373, May 2018.

[17] S. Chouhan and L. Malviya, "Four-port shared rectangular radiator with defected ground for wireless application," *Int. J. Commun. Syst.*, vol. 33, no. 9, Jun. 2020, Art. no. e4356.

[18] S. Chouhan, D. K. Panda, and V. S. Kushwah, "Modified circular common element four-port multiple-input-multiple-output antenna using diagonal parasitic element," *Int. J. RF Microw. Comput.-Aided Eng.*, vol. 29, no. 2, Feb. 2019, Art. no. e21527.

[19] A. Moradikordalivand, C. Y. Leow, T. A. Rahman, S. Ebrahimi, and T. H. Chua, "Wideband MIMO antenna system with dual polarization for WiFi and LTE applications," *Int. J. Microw. Wireless Technol.*, vol. 8, no. 3, pp. 643–650, May 2016.

[20] M. Khan, A. Capobianco, S. Asif, A. Iftikhar, B. Ijaz, and B. Braaten, "Compact 4×4 UWB-MIMO antenna with WLAN band rejected operation," *Electron. Lett.*, vol. 51, no. 14, pp. 1048–1050, 2015.

[21] A. A. Megahed, M. Abdelazim, E. H. Abdelhay, and H. Y. Soliman, "Sub-6GHz highly isolated wideband MIMO antenna arrays," *IEEE Access*, vol. 10, pp. 19875–19889, 2022.

[22] S. Ahmad, S. Khan, B. Manzoor, M. Soruri, M. Alibakhshikenari, M. Dalarsson, and F. Falcone, "A compact CPW-fed ultra-wideband multi-input-multi-output (MIMO) antenna for wireless communication networks," *IEEE Access*, vol. 10, pp. 25278–25289, 2022.

[23] A. Iqbal, A. Smida, A. J. Alazemi, M. I. Waly, N. K. Mallat, and S. Kim, "Wideband circularly polarized MIMO antenna for high data wearable biotelemetric devices," *IEEE Access*, vol. 8, pp. 17935–17944, 2020.

[24] N. Agrawal, M. Gupta, and S. Chouhan, "Modified ground and slotted MIMO antennas for 5G sub-6 GHz frequency bands," *Int. J. Microw. Wireless Technol.*, pp. 1–9, Jul. 2022.

[25] R. Krishnamoorthy, A. Desai, R. Patel, and A. Grover, "4 element compact triple band MIMO antenna for sub-6 GHz 5G wireless applications," *Wireless Netw.*, vol. 27, no. 6, pp. 3747–3759, Aug. 2021.

[26] M. S. Sharawi, "Current misuses and future prospects for printed multiple-input, multiple-output antenna systems [wireless corner]," *IEEE Antennas Propag. Mag.*, vol. 59, no. 2, pp. 162–170, Apr. 2017.

[27] J. Liang, C. C. Chiau, X. Chen, and C. G. Parini, "Study of a printed circular disc monopole antenna for UWB systems," *IEEE Trans. Antennas Propag.*, vol. 53, no. 11, pp. 3500–3504, Nov. 2005.

[28] M. Manohar, R. S. Kshetrimayum, and A. K. Gogoi, "Printed monopole antenna with tapered feed line, feed region and patch for super wideband applications," *IET Microw., Antennas Propag.*, vol. 8, no. 1, pp. 39–45, Jan. 2014.

[29] R. B. Sadineni and P. G. Dinesha, "Design of penta-band notched UWB MIMO antenna for diverse wireless applications," *Prog. Electromagn. Res. M*, vol. 107, pp. 35–49, 2022.

[30] A. K. Singh, S. K. Mahto, and R. Sinha, "Quad element MIMO antenna for LTE/5G (sub-6 GHz) applications," *J. Electromagn. Waves Appl.*, vol. 36, no. 16, pp. 2357–2372, Nov. 2022.

[31] A. K. Singh, S. K. Mahto, and R. Sinha, "Compact super-wideband MIMO antenna with improved isolation for wireless communications," *Frequenz*, vol. 75, nos. 9–10, pp. 407–417, Oct. 2021.

[32] S. Rekha and G. S. Let, "Design and SAR analysis of wearable UWB MIMO antenna with enhanced isolation using a parasitic structure," *Iranian J. Sci. Technol., Trans. Electr. Eng.*, vol. 46, no. 2, pp. 291–301, Jun. 2022.

[33] A. A. Glazunov, A. F. Molisch, and F. Tufvesson, "Mean effective gain of antennas in a wireless channel," *IET Microw., Antennas Propag.*, vol. 3, no. 2, pp. 214–227, Mar. 2009.

[34] S. L. Loyka, "Channel capacity of MIMO architecture using the exponential correlation matrix," *IEEE Commun. Lett.*, vol. 5, no. 9, pp. 369–371, Sep. 2001.

[35] A. K. Singh, S. K. Mahto, and R. Sinha, "A miniaturized MIMO antenna for C, X, and Ku band applications," *Prog. Electromagn. Res. C*, vol. 117, pp. 31–40, 2021.

SANTOSH KUMAR MAHTO was born in Patna, India, in 1985. He received the B.Tech. degree in electronics and communication engineering from the National Institute of Science and Technology, Berhampur, India, in 2010, the M.E. degree in wireless communication from BIT Mesra, Ranchi, India, in 2012, and the Ph.D. degree in microwave engineering from the National Institute of Technology, Jamshedpur, India, in 2017.

In 2017, he joined the Department of Electronics and Communication Engineering, Indian Institute of Information Technology, Ranchi, as a Faculty Member. He is currently an Associate Member with the Institute of Engineers, India. He has published two books, four book chapters, ten papers in international conferences, and 25 research article in journal of repute. He has more than three years of teaching experience. His current research interests include microwave and millimeter wave antenna, array synthesis, soft computing, and electromagnetic wave absorbers. He received the IEEE Early Member Ship Award, International Travel Support Grant from the DST Government of India, and MHRD Government of India scholarship receiving during the M.Tech. and Ph.D. programs.

AJIT KUMAR SINGH (Member, IEEE) was born in Ghazipur, Uttar Pradesh, India, in 1993. He received the B.Tech. degree in electronics and communication engineering from Uttar Pradesh Technical University, India, in 2015, the M.Tech. degree in electronics and communication engineering from the YMCA University of Science and Technology, Haryana, India, in 2019, and the Ph.D. degree in microwave engineering from the Indian Institute of Information Technology, Ranchi, India, in 2023.

He has published four book chapters, six papers in an international conference, and seven research articles in journal of repute. His current research interests include microwave and millimeter wave antenna, THz antenna, MIMO antenna, and array antenna.

RASHMI SINHA (Member, IEEE) was born in Ranchi, Jharkhand, India, in 1972. She received the B.Sc. (Engineering) degree in electrical engineering, the M.Sc. (Engineering) degree in power electronics, and the Ph.D. degree from the National Institute of Technology, Jamshedpur, India, in 1995 and 2003, respectively.

She joined the National Institute of Technology, Jamshedpur, as a Lecturer, in 1997. She has published two books, seven book chapters, ten papers in international conferences, and 20 research articles in journal of repute. She has more than 22 years of teaching experience. Her research interests include antenna design, array synthesis, microwave, metamaterial, and soft computing.

MOHAMMAD ALIBAKHSHIKENARI (Member, IEEE) was born in Mazandaran, Iran, in February 1988. He received the Ph.D. degree (Hons.) with European Label in electronics engineering from the University of Rome "Tor Vergata," Italy, in February 2020. He was a Ph.D. Visiting Researcher with the Chalmers University of Technology, Sweden, in 2018. His training during the Ph.D. degree included a research stage with Swedish Company Gap Waves AB. He is currently with the Department of Signal Theory and Communications, Universidad Carlos III de Madrid (UC3M), Spain, as the Principal Investigator of the CONEX (CONnecting EXcellence)-Plus Talent Training Program and Marie Skłodowska-Curie Actions. He was also a Lecturer in electromagnetic fields and electromagnetic laboratory with the Department of Signal Theory and Communications (2021–2022). He received the "Teaching Excellent Acknowledgment" Certificate for the course of electromagnetic fields from vice-rector of studies with UC3M. In 2022 and 2023, he was spend industrial and academic research visiting's with SARAS Technology Company Ltd., Leeds, England; Edinburgh Napier University, Edinburgh, Scotland; and University of Bradford, Bradford, England, which are defined by CONEX-Plus Talent Training Program and Marie Skłodowska-Curie Actions as his secondment research visit plans. His research interests include electromagnetic systems, antennas and wave-propagations, metamaterials and metasurfaces, synthetic aperture radars (SAR), 5G and beyond wireless communications, multiple input multiple output (MIMO) systems, RFID tag antennas, substrate integrated waveguides (SIWs), impedance matching circuits, microwave components, millimeter-waves and terahertz integrated circuits, gap waveguide technology, beamforming matrix, and reconfigurable intelligent surfaces (RIS), which led to achieve more than 4300 citations and H-index above 42 reported by Scopus, Google Scholar, and ResearchGate. He was a recipient of the three years research grant funded by Universidad Carlos III de Madrid and the European Union's Horizon 2020 Research and Innovation Program under the Marie Skłodowska-Curie Grant started, in July 2021, the two years research grant funded by the University of Rome "Tor Vergata," in November 2019, the three years Ph.D. scholarship funded by the University of Rome "Tor Vergata," in November 2016, and the two Young Engineer Awards of the 47th and 48th European Microwave Conference were held in Nuremberg, Germany, in 2017, and Madrid, Spain, in 2018, respectively. His research article titled "High-Gain Metasurface in Polyimide On-Chip Antenna Based on CRLH-TL for Sub Terahertz Integrated Circuits" published in *Scientific Reports* was awarded as the Best Month Paper with the University of Bradford, U.K., in April 2020. He also serving as an Associate Editor for *Radio Science* and *The Journal of Engineering* (IET). He also acts as a referee in several highly reputed journals and international conferences.

SALAHUDDIN KHAN, photograph and biography not available at the time of publication.

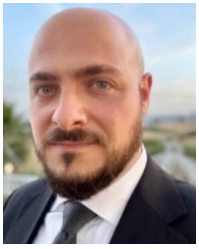

GIOVANNI PAU (Member, IEEE) received the bachelor's degree in telematic engineering from the University of Catania, Italy, and the master's degree (cum laude) in telematic engineering and the Ph.D. degree from Kore University of Enna, Italy. He is currently an Associate Professor with the Faculty of Engineering and Architecture, Kore University of Enna. He is the author/coauthor of more than 80 refereed articles published in journals and conference proceedings. His research interests include wireless sensor networks, fuzzy logic controllers, intelligent transportation systems, the Internet of Things, smart homes, and network security. He is a member of the IEEE (Italy Section) and has been involved in several international conferences as the session co-chair and a technical program committee member. He serves/served as a leading guest editor in special issues of several international journals. He also serves as an Editorial Board Member/Associate Editor for several journals, such as IEEE Access, *Wireless Networks* (Springer), *EURASIP Journal on Wireless Communications and Networking* (Springer), *Wireless Communications and Mobile Computing* (Hindawi), *Sensors* (MDPI), and *Future Internet* (MDPI).

Open Access funding provided by 'Università degli Studi di Enna "KORE"' within the CRUI CARE Agreement